SCIENCE CHINA
Information Sciences

• RESEARCH PAPER •

December 2018, Vol. 61 120201:1–120201:17
https://doi.org/10.1007/s11432-018-9588-0

From CAS & CAE Members

Cooperative transportation control of multiple mobile manipulators through distributed optimization

Jie CHEN* & Shixiong KAI

Key Laboratory of Intelligent Control and Decision of Complex Systems, School of Automation, Beijing Institute of Technology, Beijing 100081*, China*

Received 15 May 2018/Accepted 8 August 2018/Published online 22 November 2018

Abstract This paper investigates the problem of distributed control of multiple redundant mobile manipulators to collectively transport an object tracking a desired trajectory with energy and manipulability optimized. To solve this optimization problem, formation control tasks are introduced as equality constraints with the variables being the velocities. In this paper, we propose a distributed proximal gradient algorithm searching for the optimal solution, with which the stability of the closed-loop system is proved. Simulations demonstrate the effectiveness of the proposed distributed optimization scheme and proximal algorithm.

Keywords multiple mobile manipulators, cooperative transportation control, motion planning, energy and manipulability, distributed optimization

Citation Chen J, Kai S X. Cooperative transportation control of multiple mobile manipulators through distributed optimization. Sci China Inf Sci, 2018, 61(12): 120201, https://doi.org/10.1007/s11432-018-9588-0

1 Introduction

Recently, cooperative control of multiple mobile manipulators, broadly applied in industrial automation [1] and object transportation tasks [2], has attracted a significant amount of attention from researchers [3–6]. Centralized methods have been proposed to accomplish motion planning and cooperative control of multiple mobile manipulators. In particular, Alonso-Mora et al. [7] divided the controller into high-level guidance and low-level control to exploit deformability during the manipulation of soft objects. Ge et al. [8] used the so-called reduced chained form method to control the force and motion of nonholonomic mobile manipulators. It has been shown that the robustness of the system was improved such that the parametric uncertainties and bounded disturbances can be compensated for and overwhelmed. In [9], a hybrid controller was proposed to squeeze force for mobile manipulators. As a byproduct, a method was also presented to compute the load-carrying capacity of manipulators.

It is worth noting that distributed control methods have the advantages of low computation burden for each agent over centralized control schemes, distributed control methods are quite appealing for tasks of multiple mobile manipulators over large-scale network systems, in which the local information is only shared with its connected neighbors. As an extension to manipulators with fixed basement, mobile manipulators were studied in [10]. Wang and Schwager [11] proposed a concept of a force-amplifying N-robot transport system to coordinate manipulation forces from a group of robots to transport a heavy

* Corresponding author (email: chenjie@bit.edu.cn)

object without communication. The concept of "object closure" from form or force closure constraints was derived to address the problem of transporting an object with multiple mobile robots [12]. In [13], the authors proposed a feedback controller by sequentially composing vector fields or behaviors to control multiple mobile manipulators to surround and transport an object. In addition, the problem of cooperative control of robotic manipulators with dynamic uncertainties was solved using a state-relied projection estimation law and a characteristic model-based distributed controller [14]. Dong et al. [15] proposed a distributed observer for followers to estimate the leader's signal without assuming all the followers know the system matrix of the leader, and developed a distributed control law that made less use of the information of the network. A consensus protocol to compensate for the unknown delays based on the networked predictive control scheme in multi-agent systems was designed in [16]. In [17], the authors proposed a distributed adaptive robust state feedback controller to solve the problem for a class nonlinear multi-agent systems with an unknown exosystem. Huang [18] studied consensus problems for linear multi-agent systems under directed switching networks. An observer-based control law using output feedback was designed to control the followers to uniformly globally exponentially track the leader in [19].

In the tasks of cooperative control for multiple redundant mobile manipulators, the energy and manipulability optimized is very important. Owing to the fact that energy consumption describes the efficiency of the system, and it is especially useful in situations that the battery capacities are limited [20, 21]. On the other hand, manipulability is an important criterion to measure the state of a manipulator to avoid the kinematic singular configuration [22]. However, only few existing results consider both energy and manipulability optimization objectives in multiple-manipulator control tasks. For example, Li et al. [23] only investigated the energy optimization whereas Jin et al. [22] only considered the manipulability optimization in a single-manipulator system. From this sense, the combination of energy and manipulability optimization in the transportation control of multiple redundant mobile manipulators is essential.

Distributed optimization, widely employed in various fields such as smart grids, unmanned aerial vehicle (UAV) tasks, and supply chain management, has been applied to controlling multiple mobile manipulators recently [24–31]. Optimization techniques have been applied to the constrained inverse kinematics problem of redundant manipulators by using the extra degrees of freedom to meet a number of secondary functional requirements such as energy or manipulability optimization [21, 32, 33]. Li et al. [23, 34] proposed optimization frameworks for cooperative control of multiple fixed manipulators at a velocity level. Zhang et al. [35] showed that velocity-level and acceleration-level redundancy-resolution schemes can be formulated as quadratic programmings, and a simple piecewise-linear dynamics solver was proposed. In [36], a simplified solver was designed based on an infinity-norm joint velocity minimization technique. In addition, different optimization solvers were designed to realize diverse control objectives [23, 34–36]. However, these results did not consider the formation shape formed by the end-effectors. Therefore, the mobile manipulators cannot grasp and transport the target object. Furthermore, the feasibility set constraints, which make the design of a distributed algorithm more difficult, were also neglected in multiple mobile manipulators optimization. Therefore, further research into advanced distributed optimization techniques to improve the system performance for multiple redundant mobile manipulators is required.

In this paper, we focus on the distributed transportation control of multiple mobile manipulators and use the redundant degrees of freedom to optimize the energy and manipulability. We propose a novel distributed optimization framework for multiple mobile manipulators in transportation to accomplish the following goals.

• Multiple mobile manipulators grasp the target object and transport it along the desired trajectory, while satisfying the formation requirement.

• The energy and manipulabilities of the manipulators are optimized in the transportation process to reduce the energy costs and avoid the occurrence of configuration singularity.

The contributions of this paper are summarized as follows.

Problem formulation. A practical transportation task by multiple mobile manipulators with formation control and path-following requirements is formulated mathematically as a distributed optimization problem, which improves the efficiency of the system in terms of the energy costs and manipulability. The

control structure is an extension to that described in [35, 36] by using the solution of the optimization problem to realize the kinematic control of a redundant manipulator. This formulation gives a new perspective for controlling multiple mobile manipulators compared with previous results in [2, 13, 37], which only involve the control techniques.

Task objectives. Energy and manipulability optimization of multiple mobile manipulators are performed in a distributed manner, which extends the results in [22, 23]. In [23], only energy optimization has been studied and manipulators may have singular configurations. In [22], only manipulability optimization has been studied in a single-manipulator system, which might result in very high energy consumption.

Algorithm design. A general distributed continuous-time proximal algorithm, a useful tool to deal with nonsmooth, constrained, large-scale, and distributed optimization problems (see [38]), is designed to solve the proposed optimization problem. The algorithm is also applicable to more general problems with feasible constraint sets or nonsmooth objective functions.

This paper is organized as follows. In Section 2, some useful preliminary knowledge is presented and the problem of multiple mobile manipulators transportation is formulated. In Section 3, a distributed proximal algorithm is proposed to solve the problem and the theoretical proof is given. In Section 4, the simulations show the effectiveness of the novel scheme and algorithm. Finally, the main conclusion of this paper is provided in Section 5.

2 Preliminaries and problem formulation

2.1 Preliminary

In this paper, the notation is fairly standard: $\mathbb{R}$ denotes the set of real numbers; $\mathbb{R}^n$ denotes the set of n-dimensional real column vectors; $\mathbb{R}^{n\times m}$ denotes the set of $n\times m$ real matrices; I_n denotes the $n\times n$ identity matrix; $(\cdot)^{\mathrm{T}}$ denotes transpose; $\mathbf{1}_n$ denotes the $n\times 1$ vector of all ones; $\mathbf{0}_n$ denotes the $n\times 1$ vector of all zeros; $A\otimes B$ is the Kronecker product of matrices A and B; $\mathrm{diag}(b)$ denotes a diagonal matrix whose k-th diagonal entry is the k-th entry of vector b; and $\|\cdot\|$ and $\nabla_\lambda L(\cdot)$ denote the Euclidean norm and the gradient of function $L(\cdot)$ with respect to λ, respectively.

Let $\Omega\subseteq\mathbb{R}^n$ be a closed and convex set. Here $P_\Omega(u)=\mathrm{argmin}\{\|v-u\|\,|\,v\in\Omega\}$ denotes the projection of a point $u\in\mathbb{R}^n$ on Ω. It follows from [39] that $(u-P_\Omega(u))^{\mathrm{T}}(v-P_\Omega(u))\leqslant 0$, $\forall v\in\Omega$, $u\in\mathbb{R}^n$. Suppose that $f(\cdot)$ is a lower semi-continuous convex function. Then the proximal operator (see [38]) of $f(\cdot)$ is $\mathrm{prox}_f(v)=\mathrm{argmin}_x\, f(x)+\frac{1}{2}\|x-v\|^2$.

Let $\partial f(x)$ denote the subgradient of convex function $f(\cdot)$ at x. Here $\partial f(x)$ is monotone, that is $(p_x-p_y)^{\mathrm{T}}(x-y)\geqslant 0$ for all x,y, $p_x\in\partial f(x)$, and $p_y\in\partial f(y)$. In addition, the proximal operator $x=\mathrm{prox}_f(v)$ is equivalent to

$$v-x\in\partial f(x). \tag{1}$$

A nonlinear dynamical system is defined as

$$\dot{x}(t)=\phi(x(t)),\quad x(0)=x_0,\quad t\geqslant 0, \tag{2}$$

where $x(t)\in\mathcal{D}\subset\mathbb{R}^n$ is the system state vector, $\mathcal{D}$ is an open set, and $\phi(\cdot):\mathcal{D}\to\mathbb{R}^n$ is Lipschitz continuous on $\mathcal{D}$.

Lemma 1 ([40, Invariance principle, Theorem 2.41])**.** Consider the nonlinear dynamical system (2). Suppose the solution $x(t)$ to (2) corresponding to an initial condition $x(0)=x_0$ is bounded for all $t\geqslant 0$. Then the positive limit set $\omega(x_0)$ of $x(t)$, $t\geqslant 0$ is a nonempty, compact, invariant, and connected set. Furthermore, $x(t)\to\omega(x_0)$ as $t\to\infty$.

Lemma 2 ([40, Semistability, Theorem 4.20])**.** Consider the nonlinear dynamical system (2) and let $\mathcal{Q}$ be an open neighborhood of $\phi^{-1}(0)$. Suppose the orbit $\mathcal{O}_x$ of (2) is bounded for all $x\in\mathcal{Q}$ and assume that there exists a continuously differentiable function $V:\mathcal{Q}\to\mathbb{R}$ such that

$$\nabla V^{\mathrm{T}}(x)\phi(x)\leqslant 0,\quad x\in\mathcal{Q}.$$

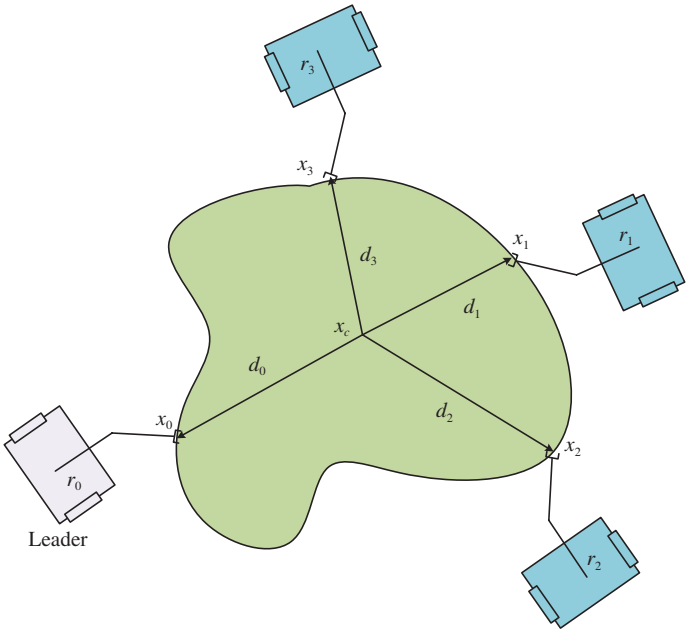

Figure 1 (Color online) Transportation task of multiple mobile manipulators.

If every point in the largest invariant subset of $\mathcal{M}$ of $\{x \in \mathcal{Q} : \nabla V^{\mathrm{T}}(x)\phi(x) = 0\}$ is Lyapunov stable, then (2) converges to a Lyapunov stable equilibrium point.

2.2 Description of multiple mobile manipulators

2.2.1 *Kinematics of a redundant mobile manipulator*

Consider multiple redundant mobile manipulators shown in Figure 1. Each mobile manipulator is composed of a manipulator arm with m joints whose positions are represented by $\theta = [\theta^1, \theta^2, \ldots, \theta^m]^{\mathrm{T}} \in \mathbb{R}^m$ and a mobile platform with the configuration $r \in \mathbb{R}^k$ working in a k-dimensional Cartesian space ($m > k$). The end-effector's Cartesian coordinate $x \in \mathbb{R}^k$ in the working space can be obtained from a nonlinear mapping

$$x(t) = r(t) + f(\theta(t)), \tag{3}$$

where $f(\cdot)$ is a nonlinear mapping from joint space to working space with known parameters for a given manipulator.

At the velocity level, calculating the time derivative of both sides of (3), we arrive at

$$v(t) = \dot{r}(t) + J(\theta(t))\omega(t), \tag{4}$$

where $v(t) = \dot{x}(t)$ is the end-effector velocity in the working space, $\omega(t) = \dot{\theta}(t)$ is the joint angular velocity in the joint space, and $J(\theta(t)) = \partial f/\partial\theta \in \mathbb{R}^{k\times m}$ is the Jacobian matrix of $f(\cdot)$ (abbreviated as J). For convenience, t is omitted in the rest of this paper, e.g., by writing $x(t)$ as x.

2.2.2 *Manipulability of a manipulator*

The quantitative measure of manipulability μ (see [41]) is given by

$$\mu(\theta) = \sqrt{\det(J(\theta)J(\theta)^{\mathrm{T}})}, \tag{5}$$

where $J(\theta)$ is the Jacobian matrix of $f(\cdot)$ and $\det(\cdot)$ is the determinant of a matrix. If the manipulator is singular, then $\mathrm{rank}(J) < m$ and $\mu(\theta) = 0$; the maximum value of $\mu(\theta)$ is 1.

2.3 Problem formulation

In this paper, we consider distributed energy and manipulability optimization in a cooperative transportation control task using $n+1$ mobile manipulators, which are connected by a graph $\mathcal{G}_{n+1}$. A mobile manipulator with label $i=0$ is defined to be the leader who knows the desired trajectory. The states of the leader satisfies $v_0=v_d$, $x_0=x_d$, and $d_0=d_d$. The graph $\mathcal{G}_{n+1}$ is obtained through a connection from the leader $i=0$ to an undirected graph $\mathcal{G}_n$ that is formed by followers with label $i=1,2,\ldots,n$. This paper aims to propose a distributed control algorithm that achieves the following objectives.

- The centroid of the target object tracks a desired trajectory and the formation of the manipulators are kept.
- Configurations of manipulators are adjusted to optimize the energy and manipulability in the transportation process.

To achieve these objectives, we formulate a novel distributed optimization framework of distributed control of multiple mobile manipulators as

$$\min_{\omega_i\in\Omega_i, v_i\in V_i} \sum_{i=0}^{n} \frac{1}{2}c_{i1}\|\omega_i\|^2+\frac{1}{2}c_{i2}\|(v_i-J_i\omega_i)\|^2-c_{i3}\omega_i^{\mathrm{T}}\Upsilon_i, \tag{6a}$$

$$\text{s.t.}\ \ v_i=\frac{1}{\sum_{j\in N_i}a_{ij}}\sum_{j\in N_i}a_{ij}[v_j-((x_i-d_i)-(x_j-d_j))],\quad i\in\{1,\ldots,n\}, \tag{6b}$$

$$v_0=v_d, \tag{6c}$$

where $c_{i1}>0$, $c_{i2}>0$, and $c_{i3}>0$ are constant coefficients, v_i and ω_i are the velocity of the end-effector and angular velocity of joints, respectively. In addition, $v_i-J_i\omega_i$ is the velocity of the mobile platform, x_i is the Cartesian coordinate of the end-effector, $\Upsilon_i=\frac{\nabla_{\theta_i}\mu_i}{|\nabla_{\theta_i}\mu_i|}$ is the unit gradient of manipulability with $H_{im}=\frac{\partial J_i}{\partial\theta_i^m}$,

$$\Upsilon_i=\frac{(\sqrt{\det(J_iJ_i^{\mathrm{T}})}(J_i\diamondsuit\{H_{i1},H_{i2},\ldots,H_{im}\})\mathrm{vec}((J_iJ_i^{\mathrm{T}})^{-1}))}{|(\sqrt{\det(J_iJ_i^{\mathrm{T}})}(J_i\diamondsuit\{H_{i1},H_{i2},\ldots,H_{im}\})\mathrm{vec}((J_iJ_i^{\mathrm{T}})^{-1}))|},$$

and $J_i\diamondsuit\{H_{i1},H_{i2},\ldots,H_{im}\}=[\mathrm{vec}(J_iH_{i1}),\mathrm{vec}(J_iH_{i2}),\ldots,\mathrm{vec}(J_iH_{im})]$ (see [22] for more details). We define d_i as the vector from the object centroid to the contact point and N_i denotes the neighbor set of the i-th manipulator. Here a_{ij} is the (i,j)-th entry of the adjacency matrix $A_{n+1}\in\mathbb{R}^{(n+1)\times(n+1)}$. Note that $a_{ij}>0$ if $j\in N_i$ and $a_{ij}=0$ otherwise. We define Ω_i and V_i as the range of the allowed joint angular velocities in joint space and end-effector velocities in task space, respectively.

Remark 1. In the cost function (6a), the first item $\frac{1}{2}c_{i1}\|\omega_i\|^2$ indicates the kinetic energy of the manipulator's joint; the second term $\frac{1}{2}c_{i2}\|(v_i-J_i\omega_i)\|^2$ represents the kinetic energy of the mobile platform; the third item $-c_{i3}\omega_i^{\mathrm{T}}\Upsilon_i$ is used to optimize the manipulability of each manipulator. The trade-off between system energy and manipulability depends on coefficients c_{i1}, c_{i2}, and c_{i3}.

Remark 2. At the velocity level, the manipulability optimization can be formulated as a convex optimization problem that is easier to solve compared with [42], in which the manipulability is a nonconvex function with respect to joint angles.

Remark 3. The cost function can be rewritten as $\min_{\omega_i\in\Omega_i,v_i\in V_i}\sum_{i=0}^{n}\frac{1}{2}c_{i1}\|\omega_i-\frac{c_{i3}}{c_{i1}}\Upsilon_i\|^2+\frac{1}{2}c_{i2}\|(v_i-J_i\omega_i)\|^2-\frac{1}{2}\frac{c_{i3}^2}{c_{i1}}\|\Upsilon_i\|^2$, which is a quadratic function lower bounded by $-\frac{1}{2}\frac{c_{i3}^2}{c_{i1}}\|\Upsilon_i\|^2$. Hence, problem (6) has solutions if it has a feasible point.

3 Main results

3.1 Tracking properties

Lemma 3. If the leader and the communication network $\mathcal{G}_n$ formed by follower mobile manipulators are connected, the constraint (6b) implies that $v_i+(x_i-d_i)=v_d+(x_d-d_d)$ for $i=1,2,\ldots,n$.

Proof. Let L_n be the Laplacian matrix of the communication network topology $\mathcal{G}_n$ for label $i = 1, 2, \ldots, n$. The i-th row and the j-th column of L_n is l_{ij}, which is defined by

$$l_{ij} = \begin{cases} \sum\limits_{k \in N_i, k \neq 0} a_{ik}, & \text{if } i = j, \\ -a_{ij}, & \text{if } i \neq j, \end{cases} \quad i, j \in \{1, \ldots, n\}.$$

Define

$$v = \begin{bmatrix} v_0 \\ v_1 \\ \vdots \\ v_n \end{bmatrix}, \quad x = \begin{bmatrix} x_0 \\ x_1 \\ \vdots \\ x_n \end{bmatrix}, \quad d = \begin{bmatrix} d_0 \\ d_1 \\ \vdots \\ d_n \end{bmatrix}, \quad \overline{L}_n = [-b\ L_n + \mathrm{diag(b)}],$$

where $b = [b_1, \ldots, b_n]^{\mathrm{T}}$, $b_i = 1$ if $0 \in N_i$ and $b_i = 0$ otherwise for $i = 1, 2, \ldots, n$.

The constraint (6b) can be rewritten as the following compact form using Kronecker algebra:

$$(\overline{L}_n \otimes I_k)[v + (x - d)] = 0, \tag{7}$$

where $\otimes$ is the Kronecker product operator, I_k is a $k \times k$ identity matrix. Here v, x, d are vectors by stacking the v_i, x_i, d_i of all mobile manipulators into a single vector, respectively.

Note that the communication network is connected. The rank of the Laplacian matrix $\overline{L}_n$ is n. Here 0 is an eigenvalue of $\overline{L}_n$ and its right eigenvector is $\mathbf{1}_{n+1}$. Owing to (6b), there exist v', x', and d' such that $v_i + (x_i - d_i) = v' + (x' - d')$ for $i = 0, 1, 2, \ldots, n$.

Note that $v_0 + (x_0 - d_0) = v_d + (x_d - d_d)$. The constraint (6b) implies that $v_i + (x_i - d_i) = v_d + (x_d - d_d)$ for $i = 1, 2, \ldots, n$.

Theorem 1. If the leader and the communication network $\mathcal{G}_n$ formed by follower mobile manipulators are connected, the solution of the optimization (6) can make the multiple mobile manipulator system achieve consensus and track the desired trajectory.

Proof. The vector d_i from object centroid to contact point is constant, thus $\dot{d}_i = 0$. The tracking error of the i-th mobile manipulator is

$$e_i = (x_i - d_i) - (x_d - d_d), \quad i \in \{0, 1, \ldots, n\}. \tag{8}$$

Calculate the time derivative on both sides of (8):

$$\dot{e}_i = \dot{x}_i - \dot{x}_d = v_i - v_d, \quad i \in \{0, 1, \ldots, n\}. \tag{9}$$

According to the Karush–Kuhn–Tucker (KKT) condition [39], a solution of optimization (6) satisfies the constraint (6b). Based on Lemma 3, the constraint (6b) implies $v_i + (x_i - d_i) = v_d + (x_d - d_d)$, hence

$$v_i - v_d = -[(x_i - d_i) - (x_d - d_d)], \quad i \in \{0, 1, \ldots, n\}. \tag{10}$$

By combining (8)–(10), the following equation can be obtained:

$$\dot{e}_i(t) = -e_i(t), \quad i \in \{0, 1, \ldots, n\}. \tag{11}$$

By solving (11), we have

$$e_i(t) = e_i(0)e^{-t}, \quad i \in \{0, 1, \ldots, n\}, \tag{12}$$

where $e_i(0)$ is the initial error, $e_i(t) \to \mathbf{0}_k$ as $t \to \infty$. Thus, the tracking error will converge exponentially to zero.

3.2 Design of the algorithm

In this subsection, a proximal algorithm is designed to solve the optimization problem (6). The optimization can be rewritten as follows:

$$\min_{\omega_i,v_i} \sum_{i=0}^{n} \frac{1}{2}c_{i1}\|\omega_i\|^2 + \frac{1}{2}c_{i2}\|(v_i - J_i\omega_i)\|^2 - c_{i3}\omega_i^{\mathrm{T}}\Upsilon_i + g_{i1}(\omega_i) + g_{i2}(v_i), \tag{13a}$$

$$\text{s.t.} \quad v_i = \frac{1}{\sum_{j\in N_i} a_{ij}} \sum_{j\in N_i} a_{ij}[v_j - ((x_i - d_i) - (x_j - d_j))], \quad i = 1,\ldots,n, \tag{13b}$$

$$v_0 = v_d. \tag{13c}$$

In this paper, $g_{i1}(\omega_i)$, $g_{i2}(v_i)$ are indicator functions of closed convex sets Ω_i, V_i, so $g_{i1}(\omega_i)$, $g_{i2}(v_i)$ are equivalent to set constraints $\omega_i \in \Omega_i$, $v_i \in V_i$. In fact, our design is valid as long as $g_{i1} : \mathbb{R}^m \to \mathbb{R}$ and $g_{i2} : \mathbb{R}^k \to \mathbb{R}$ are proper convex closed functions. The results in this paper are feasible for more general cases.

For the ease of analysis, we give the compact form of problem (13) as

$$\min_{\omega,v} f_1(\omega) + f_2(\omega, v) + f_3(\omega) + g_1(\omega) + g_2(v), \tag{14a}$$

$$\text{s.t.} \quad L[v + (x - d)] = k, \tag{14b}$$

where

$$f_1(\omega) = \sum_{i=0}^{n} \frac{1}{2}c_{i1}\|\omega_i\|^2, \quad f_2(\omega, v) = \sum_{i=0}^{n} \frac{1}{2}c_{i2}\|(v_i - J_i\omega_i)\|^2, \quad f_3(\omega) = \sum_{i=0}^{n} -c_{i3}\omega_i^{\mathrm{T}}\Upsilon_i,$$

$$g_1(\omega) = \sum_{i=0}^{n} g_{i1}(\omega_i), \quad g_2(v) = \sum_{i=0}^{n} g_{i2}(v_i),$$

$$\omega = \begin{bmatrix} \omega_0 \\ \omega_1 \\ \vdots \\ \omega_n \end{bmatrix}, \ \lambda = \begin{bmatrix} \lambda_0 \\ \lambda_1 \\ \vdots \\ \lambda_n \end{bmatrix}, \ \overline{C}_j = \begin{bmatrix} c_{0j} & 0 & 0 & 0 \\ 0 & c_{1j} & 0 & 0 \\ 0 & 0 & \ddots & 0 \\ 0 & 0 & 0 & c_{nj} \end{bmatrix}, \ J = \begin{bmatrix} J_0 & 0 & 0 & 0 \\ 0 & J_1 & 0 & 0 \\ 0 & 0 & \ddots & 0 \\ 0 & 0 & 0 & J_n \end{bmatrix},$$

$$\Upsilon = \begin{bmatrix} \Upsilon_0 \\ \Upsilon_1 \\ \vdots \\ \Upsilon_n \end{bmatrix}, \ k = \begin{bmatrix} v_d + (x_d - d_d) \\ 0 \\ \vdots \\ 0 \end{bmatrix}, \ \overline{L} = \begin{bmatrix} 1 & \mathbf{0}_{1\times n} \\ -b & L_n + \mathrm{diag}(b) \end{bmatrix},$$

$b = [b_1,\ldots,b_n]^{\mathrm{T}}$, $b_i = 1$ if $0 \in N_i$ and $b_i = 0$ otherwise for $i = 1,2,\ldots,n$, $C_1 = \overline{C}_1 \otimes I_m$, $C_2 = \overline{C}_2 \otimes I_k$, $C_3 = \overline{C}_3 \otimes I_k$, and $L = \overline{L} \otimes I_k$.

The Lagrangian function of problem (14) is defined as

$$L(\omega, v, \lambda) = \frac{1}{2}\omega^{\mathrm{T}}C_1\omega + \frac{1}{2}(v - J\omega)^{\mathrm{T}}C_2(v - J\omega) + \omega^{\mathrm{T}}C_3\Upsilon + \lambda^{\mathrm{T}}\{L[v + (x - d)] - k\} + g_1(\omega) + g_2(v),$$

where $\lambda = [\lambda_0^{\mathrm{T}}, \lambda_1^{\mathrm{T}}, \ldots, \lambda_n^{\mathrm{T}}]^{\mathrm{T}}$ is the Lagrange multiplier.

Assumption 1. (i) The weighted graph $\mathcal{G}_{n+1}$ is connected and $\mathcal{G}_n$ is undirected; (ii) Slater's condition of problem (14) holds.

Under the Assumption 1 and based on the KKT condition (see [39]) of convex optimization, there exists λ^* such that the optimal solution of the problem (14) satisfies

$$\mathbf{0}_{mn} \in -C_1\omega^* + C_2J^{\mathrm{T}}(v^* - J\omega^*) + C_3\Upsilon - \partial g_1(\omega^*), \tag{15a}$$

$$\mathbf{0}_{kn} \in -C_2(v^* - J\omega^*) - L^{\mathrm{T}}\lambda^* - \partial g_2(v^*), \tag{15b}$$

$$k = L[v^* + (x - d)], \tag{15c}$$

where ω_i^*, v_i^* for $i = 0, 1, \ldots, n$ are the optimal solution to optimization problem (14).

Note that Eq. (15) can be equivalently written in the following form (16) with the aid of proximal operators. We have Lemma 4.

Lemma 4. Under Assumption 1, a feasible point (ω^*, v^*) is the optimal solution of problem (14) if and only if there exists λ^* such that

$$\mathbf{0}_{mn} = \mathrm{prox}_{g_1}[(1 - C_1)\omega^* + C_2 J^{\mathrm{T}}(v^* - J\omega^*) + C_3\Upsilon] - \omega^*, \tag{16a}$$

$$\mathbf{0}_{kn} = \mathrm{prox}_{g_2}[(1 - C_2)v^* + C_2 J\omega^* - L^{\mathrm{T}}\lambda^*] - v^*, \tag{16b}$$

$$k = L[v^* + (x - d)]. \tag{16c}$$

The proof is a direct sequence of the KKT condition and the property of proximal operators (1).

Then, a distributed proximal algorithm is proposed as follows:

$$\dot{\omega} = \mathrm{prox}_{g_1}[(1 - C_1)\omega + C_2 J^{\mathrm{T}}(v - J\omega) + C_3\Upsilon] - \omega, \tag{17a}$$

$$\dot{v} = \mathrm{prox}_{g_2}[(1 - C_2)v + C_2 J\omega - L^{\mathrm{T}}\lambda] - v, \tag{17b}$$

$$\dot{\lambda} = L[v + \dot{v} + (x - d)]. \tag{17c}$$

Algorithm (17) uses the proximal method and derivative feedback. It is a primal–dual method to solve saddle points of the Lagrangian function $L(\omega, v, \lambda)$.

Remark 4. In algorithm (17), the contents of communication between the leader and connected followers are different. The followers receive velocities, the position, and the Lagrange multiplier from the leader. However, the leader only receives Lagrange multipliers from connected followers.

Remark 5. Like [23, 35], this algorithm recursively employs the previous solution as the new initial value in the next step. By using the previous solution, the algorithm can converge quickly because the system evolves around the equilibrium point.

3.3 Algorithm convergence

In this subsection, the convergence of the distributed proximal algorithm (17) is proved theoretically.

Theorem 2. Under Assumption 1, $(\omega^*, v^*, \lambda^*)$ is an equilibrium of algorithm (17) if and only if (ω^*, v^*) is a solution to problem (14).

Proof. An equilibrium $(\omega^*, v^*, \lambda^*)$ of algorithm (17) satisfies (16). Based on Lemma 4, $(\omega^*, v^*, \lambda^*)$ is an equilibrium of algorithm (17) if and only if (ω^*, v^*) is a solution to problem (14).

Theorem 3. Under Assumption 1:

(i) Any equilibrium of (17) is Lyapunov stable and the solution $(\omega(t), v(t))$ is bounded;

(ii) The trajectory $(\omega(t), v(t), \lambda(t))$ converges, and $\lim_{t\to\infty}(\omega(t), v(t))$ is a solution to problem (14).

Proof. (i) The Lyapunov function $V(\omega, v, \lambda)$ is constructed as

$$\begin{aligned} V = {} & \frac{1}{2}(\lambda - \lambda^*)^2 + \frac{1}{2}(\omega - \omega^*)^2 + \frac{1}{2}(v - v^*)^2 + [f_1(\omega) - f_1(\omega^*) - (\omega - \omega^*)^{\mathrm{T}}\nabla f_1(\omega^*)] \\ & + [f_2(\omega, v) - f_2(\omega^*, v^*) - (\omega - \omega^*)^{\mathrm{T}}\nabla_\omega f_2(\omega^*, v^*) - (v - v^*)^{\mathrm{T}}\nabla_v f_2(\omega^*, v^*)]. \end{aligned}$$

The function V is positive-definite, lower bounded, radically unbounded, and $\dot{V} \leqslant 0$ (see Appendix A). Therefore, $(\omega^*, v^*, \lambda^*)$ is Lyapunov stable and the trajectory $(\omega(t), v(t), \lambda(t))$ is bounded.

(ii) Define $\mathcal{R} = \{(\omega, v, \lambda) : \dot{V} = 0\} \subset \{(\omega, v, \lambda) : \dot{\omega} = 0, \dot{v} = 0\}$ (see Appendix A). Let $\mathcal{M}$ be the largest invariant set of $\mathcal{R}$. It follows from the invariant principle Lemma 1 that $(\omega(t), v(t), \lambda(t)) \to \mathcal{M}$ as $t \to \infty$ and $\mathcal{M}$ is positive invariant. Assume $(\overline{\omega}(t), \overline{v}(t), \overline{\lambda}(t))$ is a trajectory of (17) such that $(\overline{\omega}(0), \overline{v}(0), \overline{\lambda}(0)) \in \mathcal{M}$. Then $(\overline{\omega}(t), \overline{v}(t), \overline{\lambda}(t)) \in \mathcal{M}$ for all $t \geqslant 0$. Therefore, $\dot{\overline{\omega}}(t) \equiv 0, \dot{\overline{v}}(t) \equiv 0$, and

$$\dot{\overline{\lambda}}(t) \equiv L[\overline{v}(0) + (x - d)].$$

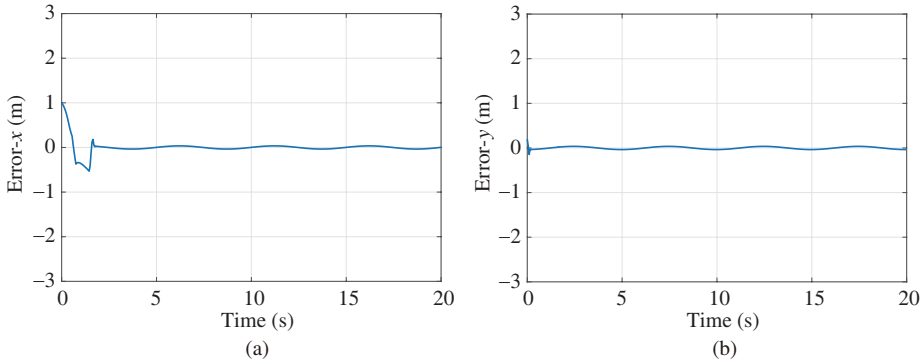

Figure 2 (Color online) Simulation results on object-tracking error using the proposed scheme (6) for transporting the object tracking a circular path. (a) Object-tracking error of the X-axis; (b) object-tracking error of the Y-axis.

Suppose $\dot{\overline{\lambda}}(t) \neq 0$. Then $\overline{\lambda}(t)$ becomes unbounded, which is a contradiction. Hence, $\mathcal{M} \subset \{(\omega, v, \lambda) : \dot{\omega} = 0, \dot{v} = 0, \dot{\lambda} = 0\}$. Note that any points in $\mathcal{M}$ is Lyapunov stable by part (i). It follows from Lemma 2 that $(\omega(t), v(t), \lambda(t))$ converges to an equilibrium point. Owing to Lemma 4, $\lim_{t\to\infty}(\omega(t), v(t))$ is a solution to problem (14).

Remark 6. The proximal algorithm (17) cannot only solve the optimization problem with set constraints, but also solve the optimization problem with nonsmooth terms in the cost function. In general, $g_1(\omega)$ and $g_2(v)$ can be convex, lower-semicontinuous, and nonsmooth functions.

4 Simulations

In this section, the efficiency of the proposed optimization scheme (6) and its proximal algorithm solver (17) are verified through numerical simulations.

4.1 Transporting an object tracking a circular path

In this subsection, four mobile manipulators cooperatively transport an object and meanwhile tracking a dynamic target point, e.g., a circular path, by using the distributed optimization scheme (6) with the solver (17). This simulation verifies the efficiency of the scheme to optimize the energy and manipulability in the process of transportation.

Parameters and initial states of four mobile manipulators are set as length $l = [1, 1]$ m, $c_{ij} = 1$ for $i = 1, 2, 3, 4$; $j = 1, 2$, and $c_{i3} = 0.6$ for $i = 1, 2, 3, 4$, initial angle $\theta_i = [0, 0.01]$ rad, initial position of mobile platform $r_1 = [2, 4]$, $r_2 = [-2, 2]$, $r_3 = [-4, -3]$, $r_4 = [4, -2]$ m, and convex sets $\Omega = [-0.5, 0.5]^2$ rad/s, $V = [-5, 5]^2$ m/s. It can be observed from the initial states that the four mobile manipulators' end-effectors are not adjacent to the object and their manipulability is low. The four end-effectors need to reach target points on the object, and then transport the object to track the desired trajectory. The object is conducted to track a circular path. To be specific, the reference of the object center moves at an angular speed at 1.25 rad/s along a circle centered at $[0, 0]$ m with radius 1 m. As observed in Figure 2, the center of the object follows the desired circular trajectory. The tracking errors of the X-axis and Y-axis almost approach zero. Figure 3 shows that the positions and velocities of four end-effectors achieve consensus. Furthermore, the formation of the end-effectors is kept during the movement.

As further demonstrated in Figure 4, the four mobile manipulators change from initial state with low manipulability to a state with high manipulability. The manipulability optimization is effective during the process of movement. The constraints of end-effector velocity and angular velocity are satisfied as shown in Figure 5. This implies that the control variables of velocity are consistent with the physical constraints.

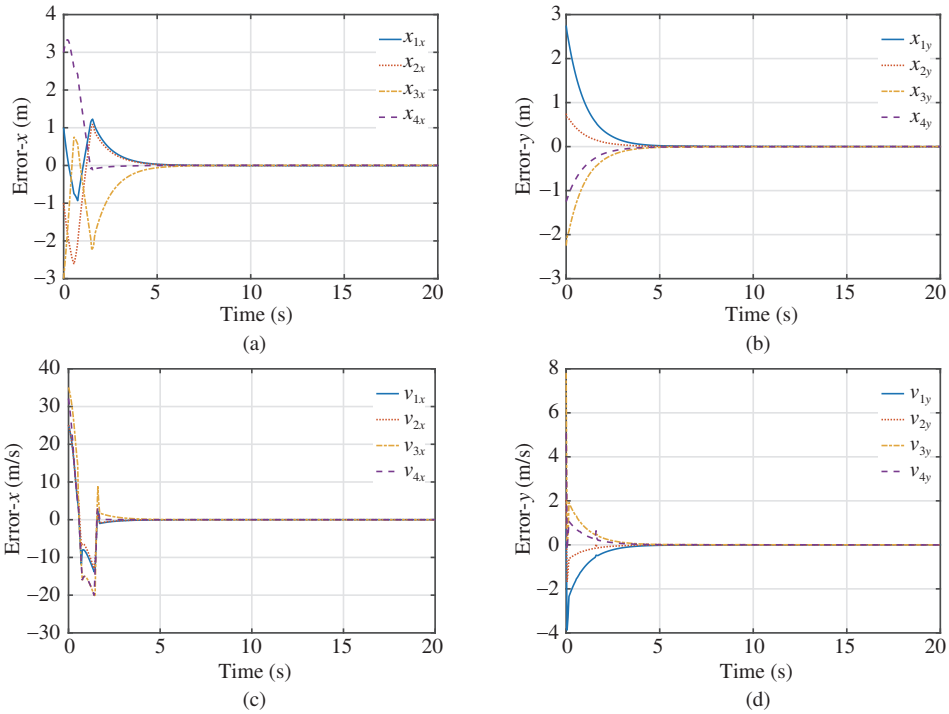

Figure 3 (Color online) Simulation results on position errors and velocity errors of end-effectors using the proposed scheme (6) for transporting the object tracking a circular path. (a) Position error of end-effectors of the X-axis; (b) position error of end-effectors of the Y-axis; (c) velocity error of end-effectors of the X-axis; (d) velocity error of end-effectors of the Y-axis.

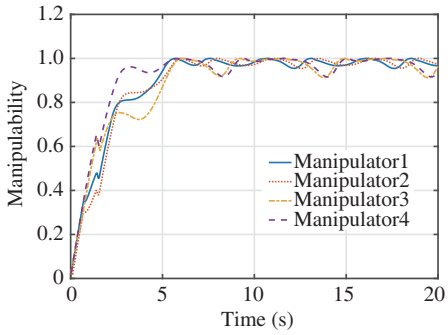

Figure 4 (Color online) Simulation results on manipulability of four mobile manipulators using the proposed scheme (6) for transporting the object tracking a circular path.

4.2 Relationship between energy and manipulability

A comparison simulation is designed to demonstrate the capability of manipulability optimization and the relationship between energy and manipulability. The first simulation uses the control scheme (6) with $c_{i3} = 0$ identifying only formation control. The second simulation uses the control scheme (6) with a constant $c_{i3} = 0.6$ for $i = 1, 2, 3, 4$ which not only has the formation control but also has manipulability optimization. The third simulation uses the same control scheme with adaptive c_{i3} as below

$$c_{i3} = \begin{cases} 1 - \mu_i, & \text{if } \mu_i < 0.5, \\ 0, & \text{if } \mu_i > 0.5, \end{cases} \quad i \in \{1, 2, 3, 4\}.$$

The physical parameters of mobile manipulators, initial states, and control objectives of these three simulations are the same as in Subsection 4.1.

As shown in Figure 6(a), the four mobile manipulators' manipulabilities fluctuate from 1 to 0 irregularly with $c_{i3} = 0$. In Figure 6(b), the four mobile manipulators' manipulabilities remain close to the

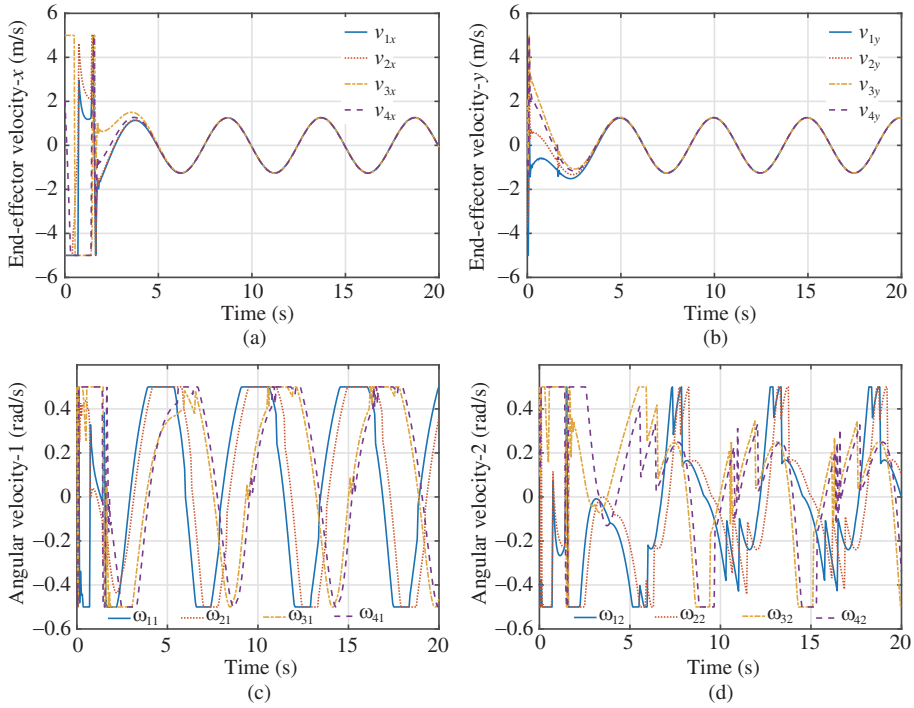

Figure 5 (Color online) Simulation results on velocity limits using the proposed scheme (6) for transporting the object tracking a circular path. (a) End-effector velocities of the X-axis; (b) end-effector velocities of the Y-axis; (c) angular velocities of joint 1; (d) angular velocities of joint 2.

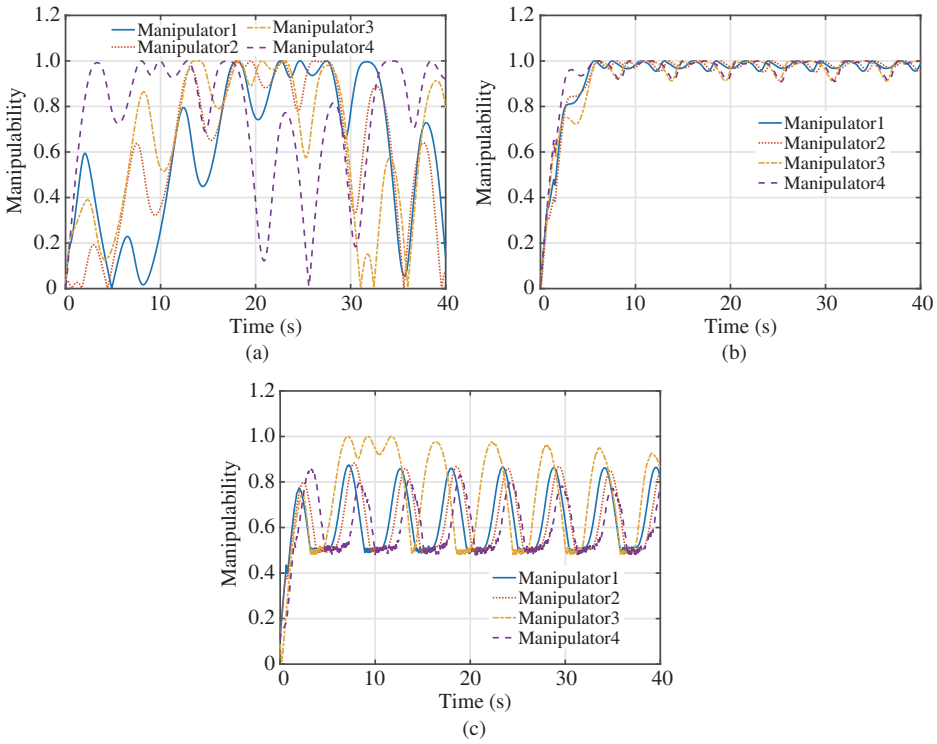

Figure 6 (Color online) Simulation results on manipulability change with different coefficients. (a) Manipulability change without manipulability optimization in the first simulation; (b) manipulability change with manipulability optimization with constant c_{i3} in the second simulation; (c) manipulability change with manipulability optimization with adaptive c_{i3} in the third simulation.

maximum value using control scheme (6) with constant c_{i3}. As illustrated in Figure 6(c), the four mobile manipulators' manipulabilities remain greater than 0.5 with adaptive c_{i3}.

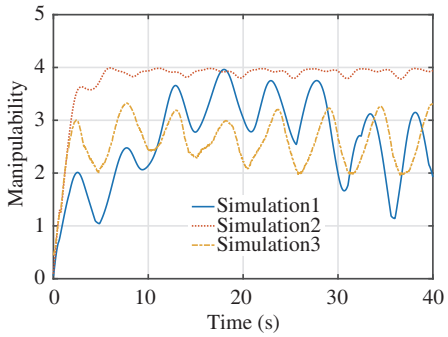

Figure 7 (Color online) Simulation results on total manipulability of four manipulators with different coefficients.

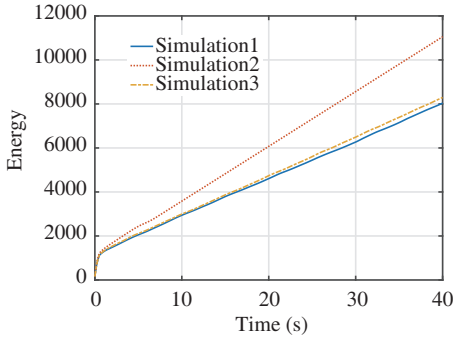

Figure 8 (Color online) Simulation results on total energy with different coefficients.

Then the total energy and manipulability of four mobile manipulators are compared. As shown in Figure 7, the manipulability on average of the second simulation is 41.36% higher than that of the first simulation. This result shows the efficiency of manipulability optimization. However, as observed in Figure 8, the energy of the second simulation is 37.52% higher than that of the first simulation. The reason is that the second simulation requires some extra energy to increase the manipulability. Furthermore, if it only needs to keep the manipulability greater than 0.5, the third simulation strikes a trade-off between energy and manipulability.

5 Conclusion

In this paper, a novel distributed transportation control scheme for multiple mobile manipulators has been proposed through distributed optimization. A distributed optimization formulation has been established by treating the formation requirement of end-effectors, physical limits of velocities, energy and manipulability as an equality constraint, feasible set constraints, and the objective function, respectively. The trade-off between system energy and manipulability was balanced under the proposed optimization framework. Then a continuous-time proximal gradient algorithm was designed to solve the proposed optimization problem. The proposed algorithm can also solve more general optimization problems with nonsmooth cost functions. The efficiency of the proposed optimization framework and algorithm has been demonstrated by simulations. In the future, game theory will be introduced to gain the largest payoff in cooperative transportation control, and transportation control in a complex environment with obstacles will be further investigated.

Acknowledgements This work was supported in part by National Natural Science Foundation of China (Grant Nos. 61621063, 61573062, 61603094), in part by Program for Changjiang Scholars and Innovative Research Team in University (Grant No. IRT1208), in part by Beijing Education Committee Cooperation Building Foundation Project (Grant No. 2017CX02005), and in part by Beijing Advanced Innovation Center for Intelligent Robots and Systems (Beijing Institute of Technology), Key Laboratory of Biomimetic Robots and Systems (Beijing Institute of Technology), Ministry of Education, Beijing, China. The authors wished to thank Prof. Hao FANG, Dr. Xianlin ZENG, and Dr. Qingkai YANG for constructive comments and suggestions.

References

1 Huntsberger T L, Trebi-Ollennu A, Aghazarian H, et al. Distributed control of multi-robot systems engaged in tightly coupled tasks. Auton Robot, 2004, 17: 79–92
2 Farivarnejad H, Wilson S, Berman S. Decentralized sliding mode control for autonomous collective transport by multi-robot systems. In: Proceedings of IEEE Conference on Decision and Control, Las Vegas, 2016. 1826–1833
3 Yoshikawa T. Foundations of Robotics: Analysis and Control. Cambridge: The MIT Press, 1990
4 Li Z J, Ge S S. Fundamentals in Modeling and Control of Mobile Manipulators. Boca Raton: CRC Press, 2013

5 Abeygunawardhana P K W, Murakami T. Vibration suppression of two-wheel mobile manipulator using resonance-ratio-control-based null-space control. IEEE Trans Ind Electron, 2010, 57: 4137–4146
6 Wei W, Mbede J B, Huang X H, et al. Neuro-fuzzy and model-based motion control for mobile manipulator among dynamic obstacles. Sci China Ser F-Inf Sci, 2003, 46: 14–30
7 Alonso-Mora J, Knepper R, Siegwart R, et al. Local motion planning for collaborative multi-robot manipulation of deformable objects. In: Proceedings of IEEE International Conference on Robotics and Automation, Seattle, 2015. 5495–5502
8 Li Z, Ge S S, Adams M, et al. Robust adaptive control of uncertain force/motion constrained nonholonomic mobile manipulators. Automatica, 2008, 44: 776–784
9 Tinos R, Terra M H, Ishihara J Y. Motion and force control of cooperative robotic manipulators with passive joints. IEEE Trans Control Syst Technol, 2006, 14: 725–734
10 Khatib O, Yokoi K, Chang K, et al. Coordination and decentralized cooperation of multiple mobile manipulators. J Robotic Syst, 1996, 13: 755–764
11 Wang Z J, Schwager M. Force-amplifying N-robot transport system (force-ANTS) for cooperative planar manipulation without communication. Int J Robot Res, 2016, 35: 1564–1586
12 Pereira G A S, Campos M F M, Kumar V. Decentralized algorithms for multi-robot manipulation via caging. Int J Robot Res, 2004, 23: 783–795
13 Fink J, Hsieh M A, Kumar V. Multi-robot manipulation via caging in environments with obstacles. In: Proceedings of IEEE International Conference on Robotics and Automation, Pasadena, 2008. 1471–1476
14 Wang L J, Meng B. Characteristic model-based consensus of networked heterogeneous robotic manipulators with dynamic uncertainties. Sci China Tech Sci, 2016, 59: 63–71
15 Dong Y, Chen J, Huang J. A self-tuning adaptive distributed observer approach to the cooperative output regulation problem for networked multi-agent systems. Int J Control, 2017. doi: 10.1080/00207179.2017.1411610
16 Liu X Y, Dou L H, Sun J. Consensus for networked multi-agent systems with unknown communication delays. J Franklin I, 2016, 53: 4176–4190
17 Dong Y, Chen J, Huang J. Cooperative robust output regulation for second-order nonlinear multiagent systems with an unknown exosystem. IEEE Trans Autom Control, 2018, 63: 3418–3425
18 Huang J. The consensus for discrete-time linear multi-agent systems under directed switching networks. IEEE Trans Autom Control, 2017, 62: 4086–4092
19 Yang Q K, Fang H, Chen J, et al. Distributed global output-feedback control for a class of Euler-Lagrange systems. IEEE Trans Autom Control, 2017, 62: 4855–4861
20 Li S, Zhang Y N, Jin L. Kinematic control of redundant manipulators using neural networks. IEEE Trans Neural Netw Learn Syst, 2017, 28: 2243–2254
21 Cai B H, Zhang Y N. Different-level redundancy-resolution and its equivalent relationship analysis for robot manipulators using gradient-descent and Zhang's neural-dynamic methods. IEEE Trans Ind Electron, 2012, 59: 3146–3155
22 Jin L, Li S, La H M, et al. Manipulability optimization of redundant manipulators using dynamic neural networks. IEEE Trans Ind Electron, 2017, 64: 4710–4720
23 Li S, He J B, Li Y M, et al. Distributed recurrent neural networks for cooperative control of manipulators: a game-theoretic perspective. IEEE Trans Neural Netw Learn Syst, 2017, 28: 415–426
24 Liang S, Zeng X L, Hong Y G. Distributed nonsmooth optimization with coupled inequality constraints via modified lagrangian function. IEEE Trans Autom Control, 2018, 63: 1753–1759
25 Liu Q S, Wang J. A second-order multi-agent network for bound-constrained distributed optimization. IEEE Trans Autom Control, 2015, 60: 3310–3315
26 Zeng X L, Yi P, Hong Y G. Distributed continuous-time algorithm for constrained convex optimizations via nonsmooth analysis approach. IEEE Trans Autom Control, 2017, 62: 5227–5233
27 Yi P, Hong Y G, Liu F. Distributed gradient algorithm for constrained optimization with application to load sharing in power systems. Syst Control Lett, 2015, 83: 45–52
28 Tang C B, Li X, Wang Z, et al. Cooperation and distributed optimization for the unreliable wireless game with indirect reciprocity. Sci China Inf Sci, 2017, 60: 110205
29 Chen J, Gan M G, Huang J, et al. Formation control of multiple Euler-Lagrange systems via null-space-based behavioral control. Sci China Inf Sci, 2016, 59: 010202
30 Li C H, Zhang E C, Jiu L, et al. Optimal control on special Euclidean group via natural gradient algorithm. Sci China Inf Sci, 2016, 59: 112203
31 Fang H, Shang C S, Chen J. An optimization-based shared control framework with applications in multi-robot systems. Sci China Inf Sci, 2018, 61: 014201
32 Taghirad H D, Bedoustani Y B. An analytic-iterative redundancy resolution scheme for cable-driven redundant parallel manipulators. IEEE Trans Robot, 2011, 27: 1137–1143
33 Patchaikani P K, Behera L, Prasad G. A single network adaptive critic-based redundancy resolution scheme for robot manipulators. IEEE Trans Ind Electron, 2012, 59: 3241–3253
34 Li S, Chen S F, Liu B, et al. Decentralized kinematic control of a class of collaborative redundant manipulators via recurrent neural networks. Neurocomputing, 2012, 91: 1–10
35 Zhang Y, Ge S S, Lee T H. A unified quadratic-programming-based dynamical system approach to joint torque optimization of physically constrained redundant manipulators. IEEE Trans Syst Man Cybern B, 2004, 34: 2126–2132
36 Tang W S, Wang J. A recurrent neural network for minimum infinity-norm kinematic control of redundant manipulators

with an improved problem formulation and reduced architecture complexity. IEEE Trans Syst Man Cybern B, 2001, 31: 98–105
37 Gueaieb W, Karray F, Al-Sharhan S. A robust hybrid intelligent position/force control scheme for cooperative manipulators. IEEE/ASME Trans Mechatron, 2007, 12: 109–125
38 Parikh N, Boyd S. Proximal algorithms. Found Trend Opt, 2013, 1: 127–239
39 Boyd S, Vandenberghe L. Convex Optimization. Cambridge: Cambridge University Press, 2004
40 Haddad W M, Chellaboina V. Nonlinear Dynamical Systems and Control: A Lyapunov-Based Approach. Princeton: Princeton University Press, 2008
41 Yoshikawa T. Manipulability of robotic mechanisms. Int J Robot Res, 1985, 4: 3–9
42 Sverdrup-Thygeson J, Moe S, Pettersen K Y, et al. Kinematic singularity avoidance for robot manipulators using set-based manipulability tasks. In: Proceedings of IEEE Conference on Control Technology and Applications, Kohala Coast, 2017. 142–149

Appendix A Convergence analysis

The algorithm (17a), (17b) can be rewritten as

$$\begin{aligned}&\dot{\omega}+\omega=\mathrm{prox}_{g_1}[(1-C_1)\omega+C_2J^{\mathrm{T}}(v-J\omega)+C_3\Upsilon],\\&\dot{v}+v=\mathrm{prox}_{g_2}[(1-C_2)v+C_2J\omega-L^{\mathrm{T}}\lambda].\end{aligned}$$

It follows from (1) that

$$(1-C_1)\omega+C_2J^{\mathrm{T}}(v-J\omega)+C_3\Upsilon-(\dot{\omega}+\omega)\in\partial g_1(\dot{\omega}+\omega),\tag{A1}$$

$$(1-C_2)v+C_2J\omega-L^{\mathrm{T}}\lambda-(\dot{v}+v)\in\partial g_2(\dot{v}+v).\tag{A2}$$

Let (ω^*,v^*,λ^*) be an equilibrium of algorithm (17). The following can be obtained:

$$-C_1\omega^*+C_2J^{\mathrm{T}}(v^*-J\omega^*)+C_3\Upsilon\in\partial g_1(\omega^*),\tag{A3}$$

$$-C_2(v^*-J\omega^*)-L^{\mathrm{T}}\lambda^*\in\partial g_2(v^*).\tag{A4}$$

Because $g_1(\cdot)$, $g_2(\cdot)$ are convex function, $\partial g_1(\cdot)$ and $\partial g_2(\cdot)$ are monotone. By combining (A1)–(A4), it follows that

$$[-C_1\omega+C_2J^{\mathrm{T}}(v-J\omega)-\dot{\omega}+C_1\omega^*-C_2J^{\mathrm{T}}(v^*-J\omega^*)]^{\mathrm{T}}(\dot{\omega}+\omega-\omega^*)\geqslant 0,\tag{A5}$$

$$[-C_2(v-J\omega)-L^{\mathrm{T}}\lambda-\dot{v}+C_2(v^*-J\omega^*)+L^{\mathrm{T}}\lambda^*]^{\mathrm{T}}(\dot{v}+v-v^*)\geqslant 0.\tag{A6}$$

According to (A5), the following is derived:

$$\begin{aligned}&(C_1\omega^*-C_1\omega)^{\mathrm{T}}(\omega-\omega^*)+[C_2J^{\mathrm{T}}(v-J\omega)-C_2J^{\mathrm{T}}(v^*-J\omega^*)]^{\mathrm{T}}(\omega-\omega^*)-\dot{\omega}^{\mathrm{T}}\dot{\omega}\\&\geqslant\dot{\omega}^{\mathrm{T}}(\omega-\omega^*)+(C_1\omega-C_1\omega^*)^{\mathrm{T}}\dot{\omega}+[C_2J^{\mathrm{T}}(v^*-J\omega^*)-C_2J^{\mathrm{T}}(v-J\omega)]^{\mathrm{T}}\dot{\omega}.\end{aligned}\tag{A7}$$

Then, (A7) is rewritten as

$$\begin{aligned}&-(\omega-\omega^*)^{\mathrm{T}}(\nabla f_1(\omega)-\nabla f_1(\omega^*))-(\omega-\omega^*)^{\mathrm{T}}(\nabla_\omega f_2(\omega,v)-\nabla_\omega f_2(\omega^*,v^*))-\dot{\omega}^{\mathrm{T}}\dot{\omega}\\&\geqslant\dot{\omega}^{\mathrm{T}}(\omega-\omega^*)+\dot{\omega}^{\mathrm{T}}(\nabla f_1(\omega)-\nabla f_1(\omega^*))+\dot{\omega}^{\mathrm{T}}(\nabla_\omega f_2(\omega,v)-\nabla_\omega f_2(\omega^*,v^*)).\end{aligned}$$

According to (A6), the following can be obtained:

$$\begin{aligned}&-[C_2J^{\mathrm{T}}(v^*-J\omega^*)-C_2J^{\mathrm{T}}(v-J\omega)]^{\mathrm{T}}(v^*-v)+(\lambda^*-\lambda)^{\mathrm{T}}L[v+\dot{v}+(x-d)]-\dot{v}^{\mathrm{T}}\dot{v}\\&\geqslant\dot{v}^{\mathrm{T}}(v-v^*)+[C_2J^{\mathrm{T}}(v-J\omega)-C_2J^{\mathrm{T}}(v^*-J\omega^*)]^{\mathrm{T}}\dot{v}.\end{aligned}\tag{A8}$$

Then, (A8) can be rewritten as

$$\begin{aligned}&-(v-v^*)^{\mathrm{T}}(\nabla_v f_2(\omega,v)-\nabla_u f_2(\omega^*,v^*))+(\lambda^*-\lambda)^{\mathrm{T}}L[v+\dot{v}+(x-d)]-\dot{v}^{\mathrm{T}}\dot{v}\\&\geqslant\dot{v}^{\mathrm{T}}(v-v^*)+\dot{v}^{\mathrm{T}}(\nabla_v f_2(\omega,v)-\nabla_v f_2(\omega^*,v^*)).\end{aligned}$$

The function $V_1(\omega,u)$ is constructed as

$$\begin{aligned}V_1=&\frac{1}{2}(\omega-\omega^*)^2+\frac{1}{2}(v-v^*)^2+[f_1(\omega)-f_1(\omega^*)-(\omega-\omega^*)^{\mathrm{T}}\nabla f_1(\omega^*)]\\&+[f_2(\omega,v)-f_2(\omega^*,v^*)-(\omega-\omega^*)^{\mathrm{T}}\nabla_\omega f_2(\omega^*,v^*)-(v-v^*)^{\mathrm{T}}\nabla_v f_2(\omega^*,v^*)].\end{aligned}\tag{A9}$$

Computing time derivative of V_1 in (A9), the following can be derived:

$$\begin{aligned}\dot{V}_1=&\dot{\omega}^{\mathrm{T}}(\omega-\omega^*)+\dot{\omega}^{\mathrm{T}}(\nabla f_1(\omega)-\nabla f_1(\omega^*))+\dot{\omega}^{\mathrm{T}}(\nabla_\omega f_2(\omega,v)-\nabla_\omega f_2(\omega^*,v^*))\\&+\dot{v}^{\mathrm{T}}(v-v^*)+\dot{v}^{\mathrm{T}}(\nabla_v f_2(\omega,v)-\nabla_v f_2(\omega^*,v^*))\\\leqslant&-(\omega-\omega^*)^{\mathrm{T}}[\nabla f_1(\omega)-\nabla f_1(\omega^*)]\\&-(\omega-\omega^*)^{\mathrm{T}}[\nabla_\omega f_2(\omega,v)-\nabla_\omega f_2(\omega^*,v^*)]\\&-(v-v^*)^{\mathrm{T}}[\nabla_v f_2(\omega,v)-\nabla_v f_2(\omega^*,v^*)]\end{aligned}$$

$$+ (\lambda^* - \lambda)^{\mathrm{T}} L[v + \dot{v} + (x - d)] - \dot{\omega}^{\mathrm{T}}\dot{\omega} - \dot{v}^{\mathrm{T}}\dot{v}. \tag{A10}$$

Based on $\dot{V}_1$ (A10), another function $V_2(\lambda)$ is constructed as

$$V_2 = \frac{1}{2}(\lambda - \lambda^*)^2. \tag{A11}$$

By calculating the time derivative of V_2, $\dot{V}_2$ can be obtained

$$\dot{V}_2 = \dot{\lambda}^{\mathrm{T}}(\lambda - \lambda^*) = (\lambda - \lambda^*)^{\mathrm{T}} L[v + \dot{v} + (x - d)]. \tag{A12}$$

It follows from (A10) and (A12) that

$$\begin{aligned}
\dot{V} &= \dot{V}_1 + \dot{V}_2 \\
&\leqslant -(\omega - \omega^*)^{\mathrm{T}}[\nabla f_1(\omega) - \nabla f_1(\omega^*)] \\
&\quad - (\omega - \omega^*)^{\mathrm{T}}[\nabla_\omega f_2(\omega, v) - \nabla_\omega f_2(\omega^*, v^*)] \\
&\quad - (v - v^*)^{\mathrm{T}}[\nabla_v f_2(\omega, v) - \nabla_v f_2(\omega^*, v^*)] \\
&\quad - \dot{\omega}^{\mathrm{T}}\dot{\omega} - \dot{v}^{\mathrm{T}}\dot{v} \\
&\leqslant -\dot{\omega}^{\mathrm{T}}\dot{\omega} - \dot{v}^{\mathrm{T}}\dot{v} \\
&\leqslant 0.
\end{aligned}$$

As a result, $\{(\omega, v, \lambda) : \dot{V} = 0\} \subset \{(\omega, v, \lambda) : \dot{\omega} = 0, \dot{v} = 0\}$. In addition, because f_1 and f_2 are convex functions, then

$$\begin{aligned}
&f_1(\omega) - f_1(\omega^*) - (\omega - \omega^*)^{\mathrm{T}}\nabla f_1(\omega^*) \geqslant 0, \\
&f_2(\omega, v) - f_2(\omega^*, v^*) - (\omega - \omega^*)^{\mathrm{T}}\nabla_\omega f_2(\omega^*, v^*) - (v - v^*)^{\mathrm{T}}\nabla_v f_2(\omega^*, v^*) \geqslant 0.
\end{aligned}$$

By combining (A9) and (A11), it follows that

$$\begin{aligned}
V &= V_1 + V_2 \\
&= \frac{1}{2}(\omega - \omega^*)^2 + \frac{1}{2}(v - v^*)^2 + [f_1(\omega) - f_1(\omega^*) - (\omega - \omega^*)^{\mathrm{T}}\nabla f_1(\omega^*)] \\
&\quad + [f_2(\omega, v) - f_2(\omega^*, v^*) - (\omega - \omega^*)^{\mathrm{T}}\nabla_\omega f_2(\omega^*, v^*) - (v - v^*)^{\mathrm{T}}\nabla_v f_2(\omega^*, v^*)] + \frac{1}{2}(\lambda - \lambda^*)^2 \\
&\geqslant \frac{1}{2}(\omega - \omega^*)^2 + \frac{1}{2}(v - v^*)^2 + \frac{1}{2}(\lambda - \lambda^*)^2 \\
&\geqslant 0.
\end{aligned}$$

Profile of Jie CHEN

Prof. Chen received the B.S., M.S., and Ph.D. degrees in control theory and control engineering from the Beijing Institute of Technology, in 1986, 1996, and 2001, respectively. From 1989 to 1990, he was a visiting scholar in the California State University, USA. From 1996 to 1997, he was a research fellow in the School of E&E, the University of Birmingham, UK. From July 1986 to June 2018, he worked at the Beijing Institute of Technology. He is now the president of the Tongji University.

He has devoted more than thirty years to the field of control science and engineering. His main research interests include multi-objective optimization and decision in complex systems, multi-agent systems, intelligent control, nonlinear control, and optimization methods. He is a recipient of the Changjiang Scholars, Ministry of Education of China, and the National Science Fund for Distinguished Young Scholars. In 2017, he was elected as an academician of the Chinese Academy of Engineering.

Prof. Chen is currently the director of the State Key Laboratory of Intelligent Control and Decision of Complex Systems and the Beijing Advanced Innovation Center of Intelligent Robots and Systems. He is also a leader of the Innovative Research Groups of the National Natural Science Foundation of China. He has served as a Vice President of the Chinese Association of Automation from 2013, a Vice President of the Chinese Association of Command and Control from 2017, and the executive member of the Chinese Association for Artificial Intelligence form 2008. He has also served as the Managing Editor for the Journal of Systems Science and Complexity since 2014, Associate Editor for several journals including *IEEE Transactions on Cybernetics* and *SCIENCE CHINA Information Sciences*, and Subject Editor of *International Journal of Robust and Nonlinear Control*. He is a member of the 7th Review Panel on Control Science and Engineering, the Chinese State Council Academic Degrees Committee, and a member of the 7th Committee on Science and Technology, Ministry of Education of China.

Reveal the important mechanism on the exploration-exploitation tradeoff behind dispersion and aggregation phenomena

With rapid development of socialized production and modern war, distributed cooperative operation of manufacturing machinery and weapons is in urgent need (Xin et al., 2010; Xin et al., 2011). Distributed coordinated planning and cooperative behavior control are crucial to effective cooperation (Chen et al. 2016). Breadth-first search and depth-first search in intelligent optimization is one of the fundamental problems in distributed cooperative control, and becomes a hot and difficult topic (Chen et al., 2009; Chen et al., 2017). The exploration-exploitation tradeoff behind dispersion and aggregation phenomena also widely exists in biological populations. Prof. Chen discovered the tradeoff mechanism and proposed the optimal contraction theorem for intelligent optimization (Chen et al. 2009). The relationship between the exploration-exploitation tradeoff and problem hardness has been clarified from system optimization perspective. With his endeavor, the well-known hard problem regarding the best tradeoff between breadth-first search and depth-first search has been solved. Prof. Chen also proposed efficient mechanisms and strategies of hybridizing different biologically inspired population-based intelligent optimizers (Xin et al., 2012). Supported by National Natural Science Foundation of China (NSFC) and other foundations, a breakthrough in theories and methods of hybrid intelligent optimization has been achieved.

Reveal the coupling mechanism among dynamic model, topology, and stability of distributed systems

The past two decades have witnessed unprecedented development in artificial intelligence, within which one core research branch is the cooperative control for multi-agent systems. The inherent complexity of nonlinear dynamic models, environment uncertainties, and implicit inner couplings all bring great challenges to reveal the mechanism between distributed control and system behavior. Output feedback control for strongly nonlinear Euler-Lagrange system has been a long-term bottleneck since last century. Prof. Chen has successfully developed a novel coordinate reconstruction scheme, with which the stable mechanism has been identified (Yang et al. 2017). The fundamental principles to guarantee stability of multi-agent systems with nonlinear dynamics has also been disclosed (Chen et al. 2016). In practical applications, the systems are inevitable to be exposed in complex environments including unknown threatens. Prof. Chen have identified the influence of fault information perception on system behavior and proposed distributed fault detection strategies through local interaction (Li et al. 2018). The implicit relationships between system controllability and underlying interaction topologies has been revealed (Fang et al. 2016). Time-delay is regarded as one essential factor in affecting system's stability. Prof. Chen has discovered the stability mechanisms for networked control systems subject to time-varying delays

through aperiodic sampling and polytopic approximation techniques (Chen et al. 2017, Wang et al. 2016).

Prof. Chen has co-authored 4 books and more than 200 research papers which were published on IEEE Transactions, other top-ranked journals like Automatica. More importantly, all these theoretical studies have been successfully applied in many real projects, such as cooperative strategic decision-making and control of heterogeneous ground vehicles. His studies have been highly recognized. In fact, he has received numerous awards including one second-grade prize of the National Natural Science Award of China (2014), two second-grade prizes of the National Science and Technology Progress Award of China (2009, 2011).

Selected publications

• Chen J, Xin B, Peng Z H, et al. Optimal contraction theorem for exploration-exploitation tradeoff in search and optimization. IEEE Trans Syst Man Cybern A, 2009, 39: 680–691

• Chen J, Li J, Xin B. DMOEA-εC: decomposition-based multiobjective evolutionary algorithm with the ε-constraint framework. IEEE Trans Evolut Comput, 2017, 27: 714–730

• Chen J, Zha W Z, Peng Z H, et al. Multi-player pursuit-evasion games with one superior evader. Automatica, 2016, 71: 24–32

• Xin B, Chen J, Zhang J, et al. Hybridizing differential evolution and particle swarm optimization to design powerful optimizers: a review and taxonomy. IEEE Trans Syst Man Cybern C, 2012, 42: 744–767

• Xin B, Chen J, Peng Z H, et al. An efficient rule-based constructive heuristic to solve dynamic weapon-target assignment problem. IEEE Trans Syst Man Cybern A, 2011, 41: 598–606

• Xin B, Chen J, Peng Z H, et al. Efficient decision-makings for dynamic weapon-target assignment by virtual permutation and tabu search heuristics. IEEE Trans Syst Man Cybern C, 2010, 40: 649–662

• Yang Q K, Fang H, Chen J, et al. Distributed global output-feedback control for a class of Euler-Lagrange systems. IEEE Trans Autom Control, 2017, 62: 4855–4861

• Li Y, Fang H, Chen J. Distributed cooperative fault detection for multi-agent systems: a mixed H_∞/H_2 optimization approach. IEEE Trans Industr Electron, 2018, 65: 6468–6477

• Fang H, Wei Y, Chen J, et al. Flocking of second-order multi-agent systems with connectivity preservation based on algebraic connectivity estimation. IEEE Trans Cybern, 2017, 47: 1067–1077

• Chen J, Meng S, Sun J. Stability analysis of networked control systems with aperiodic sampling and time-varying delay. IEEE Trans Cybern, 2017, 47: 2312–2320

• Wang Z, Sun J, Chen J. A new polytopic approximation method for networked systems with time-varying delay. IEEE Trans Circuit Syst II-Express Brief, 2016, 63: 843–847

• Chen J, Gan M G, Huang J, et al. Formation control of multiple Euler-Lagrange systems via null-space-based behavioral control. Sci China Inf Sci, 2016, 59: 010202